Chapter 6
Tidal Forested Wetlands: Mechanisms, Threats, and Management Tools

Thomas Williams, Devendra Amatya, William Conner, Sudhanshu Panda, Guangjun Xu, Jihai Dong, Carl Trettin, Changming Dong, Xiaoqian Gao, Haiyun Shi, Kai Yu, and Hongjun Wang

6.1 Introduction

Tidal wetlands, occurring at the interface between terrestrial and marine systems, have high rates of productivity and biogeochemical processes driven by periodic subsidies of water and nutrients brought about by tidal water level fluctuations (Odum 1988; Day et al. 2007; Baldwin et al. 2009). These tidal wetland areas are known for performing several important ecosystem services, such as water yield and storage, flood buffering, filtering and removing/recycling pollutants, storm water protection, support of entire food webs sustaining human consumption, biodiversity conservation, recreational opportunities, and wildlife/aquatic habitat provision (Carter 1990). Forested tidal wetlands, mangroves, and tidal freshwater forested wetlands (TFFWs) represent an important subset of these valuable coastal wetlands. Barbier et al. (2011) showed that six coastal landforms (including non-wetland dune and sea grass beds) produced over US$10,000 ha^{-1} of environmental service values.

T. Williams · W. Conner
Baruch Institute of Coastal Ecology and Forest Science, Clemson University, Georgetown, SC, USA

D. Amatya (✉) · C. Trettin
USDA Forest Service, Center for Forested Wetlands Research, Santee Experimental Forest, Cordesville, SC, USA
e-mail: Devendra.M.Amatya@usda.gov

S. Panda
Institute of Environmental Spatial Analysis, University of North Georgia, Oakwood, GA, USA

G. Xu · J. Dong · C. Dong · X. Gao · H. Shi · K. Yu
Oceanic Modeling and Observation Laboratory, Nanjing University of Information Science and Technology, Nanjing, PR China

H. Wang
Duke University Wetland Center, Nicholas School of the Environment, Duke University, Durham, NC, USA

S. An, J. T. A. Verhoeven (eds.), *Wetlands: Ecosystem Services, Restoration and Wise Use*, Ecological Studies 238, https://doi.org/10.1007/978-3-030-14861-4_6

Their evaluation of mangroves included over US$13,000 ha^{-1} for coastal protection, erosion control, and fishery maintenance, plus up to US$615 ha^{-1} $year^{-1}$ for raw material production and carbon sequestration. Their evaluation concentrated only on the coastal zone proper and did not include TFFW as a separate category.

While tidal wetlands provide valuable environmental services, they are greatly threatened by land use change and sea level rise. Halpern et al. (2008) found moderate or major human impacts on 42% of the worlds coastal areas. Algoni (2002) reported that one third of the world's mangroves had been lost to human activities in the last 50 years. TFFWs with Sitka spruce (*Picea sitchensis*) in Northwestern North America have not been recognized in many compilations of TFFWs because so little of this ecosystem remains after human utilization of these wetlands (Diefenderfer et al. 2008). Sea level rise may displace many tidal wetlands with open water (Craft et al. 2009), but it is more likely that the fate of salt marshes and mangroves will be determined by a much more complex interaction of sedimentation and productivity versus decomposition and settling, in relation to the rate of sea level rise (Kirwan and Megonigal 2013). Ensign et al. (2012) suggest that TFFW may be the most vulnerable coastal wetland category due to both a decline in productivity caused by salt inundation and a low sediment input due to river hydraulics.

Both mangrove forests and TFFW are valuable wetlands that are at risk due to human development and sea level rise. This chapter cannot do justice to the large body of knowledge already accumulated on these subjects. Readers interested in the ecology and botany of mangroves will find information in Twilley and Day (2012), Tomlinson (2016), or Teas (2013). Likewise, TFFWs are the subject of Conner et al. (2007), and related information can also be found in Barendregt et al. (2009) and Batzer and Baldwin (2012) although, in general, research on this ecotone between coastal rivers and marine waters is limited. Ensign et al. (2012) stated that the tidal river represents a combination of the forces of tidal mechanics studied by oceanography and linear hydraulics of riverine floodplains which has not been specifically studied by any discipline. In this chapter, we will attempt to examine tidal and freshwater forces that are important to understanding distribution, functions, and values of tidal forests and the threats posed to these ecosystems from human development and climate change. We will also attempt to describe general and global processes with examples from our experience in the Southeastern United States and China. In addition, we will describe how new advances in remote sensing and spatial analysis have changed our ability to observe and predict these forces.

6.2 Historical to Present Understanding of the Tide and Tidal Wetlands

6.2.1 The Tides

Following a trip to what is now England in 330 BC, the Greek astronomer Pytheas described the connection of the moon to the large daily tide cycles he observed there

(Ekman 1993). Nearly 20 centuries later, Newton described scientifically how tides were driven by gravitation of the sun and the moon. In the late nineteenth century, Lord Kelvin applied Newtonian physics, Laplace mathematics, and hydraulic principles of Bernoulli to explain tidal fluctuations as harmonic waves driven by various periods of astronomical forcing. These relationships were used to develop tidal predictions until the middle twentieth century (Darwin 1901; Doodson 1921; Macmillan 1966).

Until the mid-1990s, tidal fluctuation and sea level were measured at hundreds of locations around the earth. Each gauge stage was recorded relative to a practical datum for that particular gauge, often chosen to be some depth below mean lower low water to assure navigation in the local channels. Many nations used profile leveling between the gauges to develop a national datum relative to mean sea level at those stations. In the United States, that was the National Geodetic Vertical Datum of 1929. However, the global sea surface is currently measured by satellite altimetry by the TOPEX/Poseidon and subsequent JASON series satellites (Albain et al. 2017). The GRACE (Gravity Recovery and Climate Experiment) satellites have developed maps of the gravity differences to create a global equipotential surface that can be compared to the reference ellipsoid of satellite orbits. From satellite altimetry, the range of tides can be estimated for all of the oceans of the world (Fig. 6.1). In addition to the wide range of tide heights, the period of the tide varies from diurnal

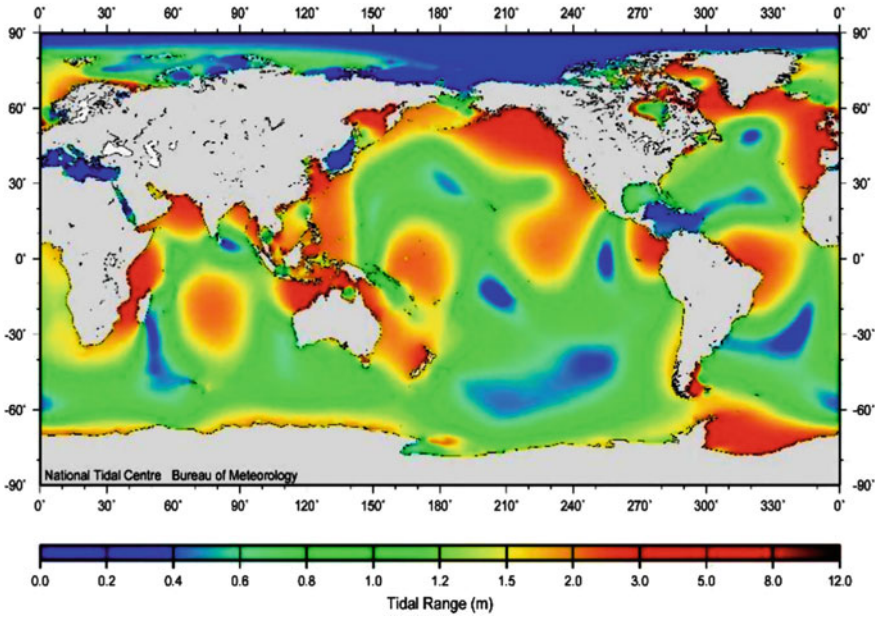

Fig. 6.1 Range of tidal fluctuation for oceans of the world. (Calculated as tidal ranges in meters from principal lunar and solar semidiurnal and diurnal harmonic amplitudes, $2\times$ (M2 + S2 + K1 + O1) from data by National Tidal Centre, Australian Bureau of Meteorology, in Matthews and Matthews (2014). Used with permission. The symbols M2, S2, K1, and O1 are standard tidal constituents)

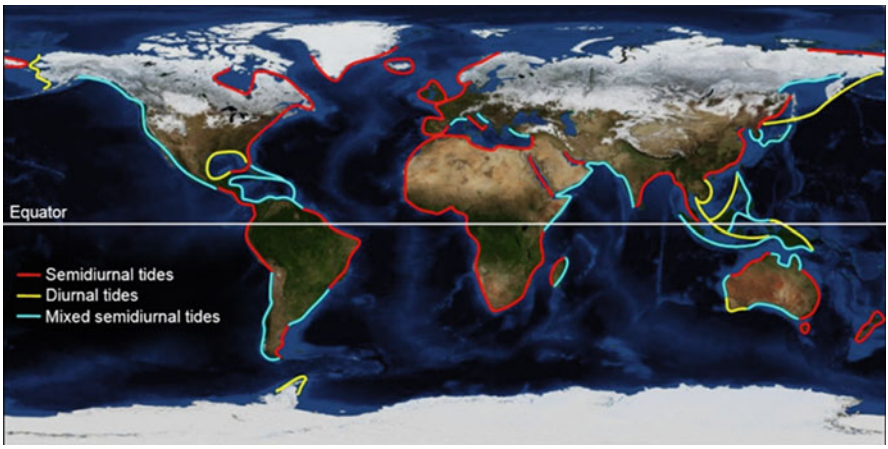

Fig. 6.2 Distribution of tidal periods across the earth (NOAA 2017)

(one tide per day) to semidiurnal (two equal tides per day) to mixed (two tides of differing amplitude and period per day) (Fig. 6.2).

6.2.2 Example of Coastal Wetland Variation Along the Eastern China Coast

Jiangsu Province, located on the eastern China coast (Lat. 33° N Long. 121° E), has the largest tidal flats in China due to large river sediment supply, gentle coastal slope, and large tidal flows (Gao 2009). Between 1127 AD and 1885 AD, the Yellow River developed a large delta (40–60 km wide) along the Jiangsu coast before the river coarse changed to the north in 1885 AD (Zhang 1984). The coastal flats have shown dynamic redistribution of sediments with erosion near the delta with redistribution and accretion along the central coast (Gao 2009).

Coastline changes and their implications to coastal wetlands variation are of great significance to environmental change in coastal zones. Many researchers have studied satellite coastline mapping in different areas of the world (Dellepiane et al. 2004; Alesheikh et al. 2007; Gens 2010; Zhang et al. 2013; Liu et al. 2016; Nunziata et al. 2016). However, developing methods to examine coastline change remains a challenge. High-resolution satellite remote sensing images [synthetic aperture radar (SAR)] and Landsat TM (Thematic Mapper) data have been used to explore coastline changes in Jiangsu and Zhejiang Provinces of China.

Images of Envisat ASAR (Advanced Synthetic Aperture Radar) produced by the European Space Agency (ESA) and Landsat TM (Thematic Mapper) produced by the National Aeronautics and Space Administration (NASA) were used in this study. The Envisat ASAR images, in image mode, possess a spatial resolution of 30 m and

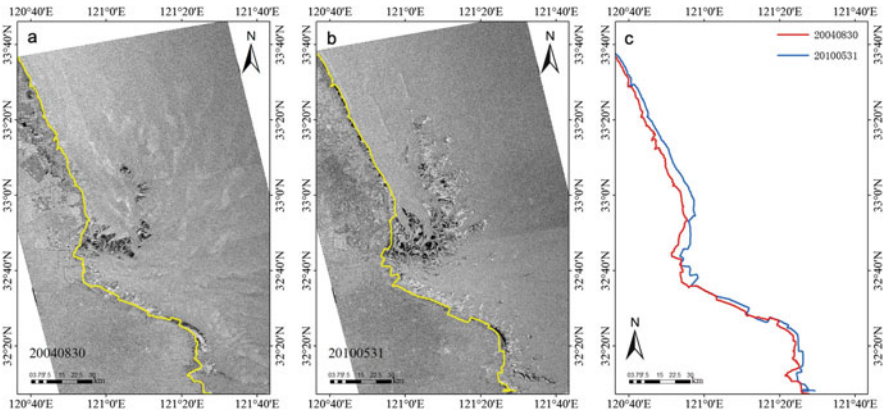

Fig. 6.3 Coastlines detected along Jiangsu Province in eastern China on August 30, 2004 (**a**) and May 31, 2010 (**b**) in Envisat SAR images. (**c**) A comparison of coastlines in 2004 with that in 2010. Yellow lines in (**a**) and (**b**) are the coastlines interpreted from ASAR data

a swath width of 100 km. TM images had a spatial resolution of 30 m. Orbit height of both satellites was 705 km and collected data for the same area once every 16 days.

In ASAR images, land and water features are depicted on a varying gray scale with the coastline defined as the place with the greatest gradient of gray scale. Figure 6.3 shows the coastal areas along Jiangsu Province in eastern China on August 30, 2004 and May 31, 2010. The coastline in 2010 was more offshore than in 2004 in the ASAR images, suggesting an accretion of sediments.

Zhejiang Province (Lat. 29° N Long. 120° E) lies south of the delta of the Yangtze River which once delivered large sediment loads, over 400 Mt year^{-1} (Chen et al. 1985), to the coastal region. However, human management impacts, primarily completion of the Three Gorges Dam in 2003, have reduced sediment transport to the coast by 70% and are expected to decrease transport even more, to approximately 110 Mt year^{-1} by 2050 (Yang et al. 2014). Understanding the impact of these changes to the coastal systems is an area of great concern.

The coastal changes of Zhejiang Province can be clearly shown by comparing TM images, in which the difference between land and sea water is more obvious in the near-infrared image (Band 5 of TM images) (Fig. 6.4). Apparent coastline movement, to both the west and the east, between 1984, 1990, 1995, 2001, and 2015 images (Fig. 6.5) indicates both positive (east) and negative (west) changes in coastal area with no obvious trend.

These findings reveal a major difficulty in satellite-based wetland mapping of the western coastline of the East China Sea. This region has strong semidiurnal tidal fluctuations (Fig. 6.1) with a mean tidal range of 2.66 m and a maximum range of 4.62 m in the Yangtze Estuary (Luan et al. 2016). Land slopes of the coastal region are very flat, 0.00010 to 0.0005 (Gao 2009), allowing large lateral movements of the water's edge over the tidal range. In order to use satellite data to determine influences of human impact, a tidal correction must be applied to each scene analyzed.

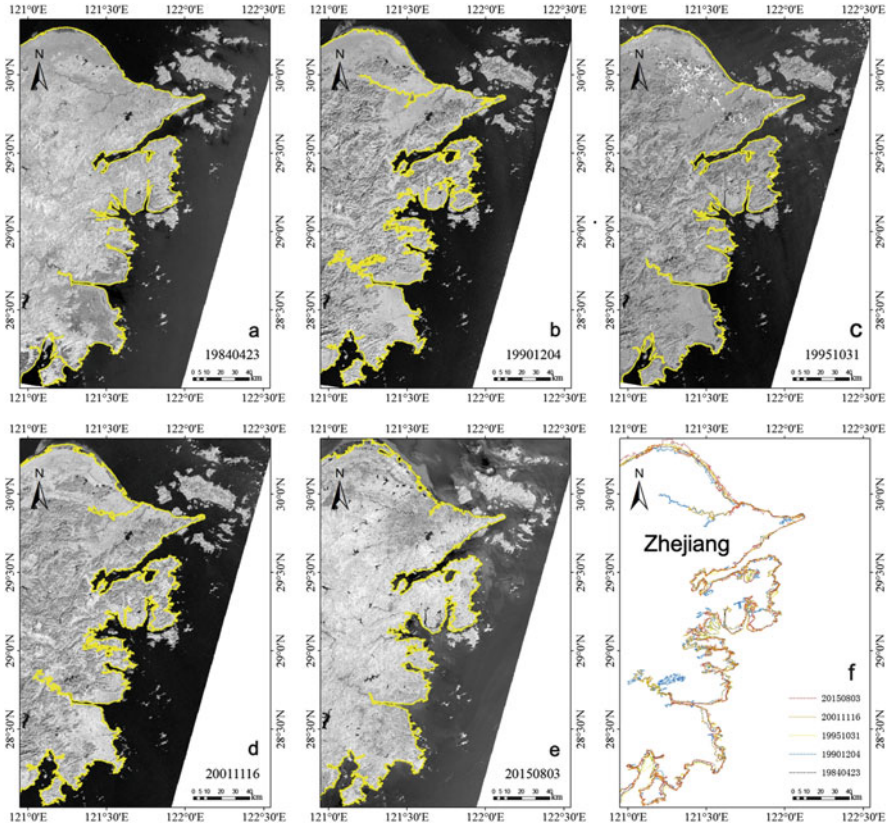

Fig. 6.4 Coastlines detected along Zhejiang Province in eastern China on April 23, 1984 (**a**), December 04, 1990 (**b**), October 31, 1995 (**c**), November 16, 2001 (**d**), and August 03, 2015 (**e**) in TM images. (**f**) Comparison of coastlines extracted from TM images. Yellow lines mark the extracted coastlines

Hydrodynamic models are generally used to predict tidal elevations over oceanic regions. A modern hydrodynamic model is essentially an extension of the analytic models first proposed by Lord Kelvin in the late nineteenth century. The development of high speed computing has allowed numerical approximations of the differential equations describing water movement dynamics that include terms to define changes in gradient, density, salinity, wind shear, bottom friction, and basin geometry which cannot be solved analytically. The Princeton Ocean Model (Blumberg and Mellor 1987) is such a numerical model that has been widely used and modified to study ocean basins around the world. Song et al. (2013) used a variation of that model, modified for parallel computer processing (Jordi and Wang 2012) and wetting and drying of tidal flats (Oey 2005), to model the entire East China Sea. The model was integrated for 56 years (1955–2010) with a full range of dynamic forces, including tides, sea surface fluxes of momentum, heat, and

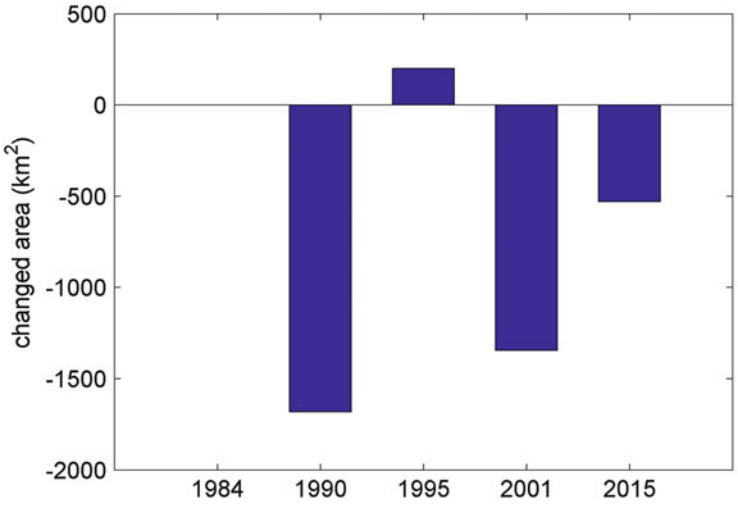

Fig. 6.5 Time series of changed area along Zhejiang Province compared to the 1984 situation using TM images

freshwater, lateral flux (see Fig. 6.6a, b for the model domain). The power spectrum of the wetland area has several peaks at different periods, ranging from hours to decades.

The anomaly from the mean value can be viewed as the variation of wetland area, indicating the difference in dry land between flood and ebb tide. Positive variation indicates an emerging wetland and lower tide, while negative variation indicated rising tide and submerging land. Generally, these peaks can be classified into nine bands: high-frequency (less than half day), semidiurnal, diurnal, semimonthly, monthly, semiannual, annual, interannual (3–10 years), and decadal (>10 years). Overall, the range in variation of the wetland, about 5000 km^2, demonstrates the very large intertidal wetlands found along the coast of Jiangsu Province and the large differences that may occur in satellite images from differing stages of the tide.

6.3 From the Ocean to Upland: Modeling Water Levels

In the preceding example, ocean tides directly impacted the extent of coastal tidal wetlands. The semidiurnal component contributed to more than 60% of the total wetland variability. In shallow coastal waters, bottom friction induces significant nonlinearity, resulting in the generation of higher- and lower-frequency harmonics (Fang et al. 2004; Egbert et al. 2010). The biweekly (fortnightly) periods are caused by alignment of the sun and moon with phases in the moon. Semiannual periods are due to more linear alignment of the earth, moon, and sun during the equinoxes. Annual cycles are produced by seasonal ocean thermal expansion and atmosphere

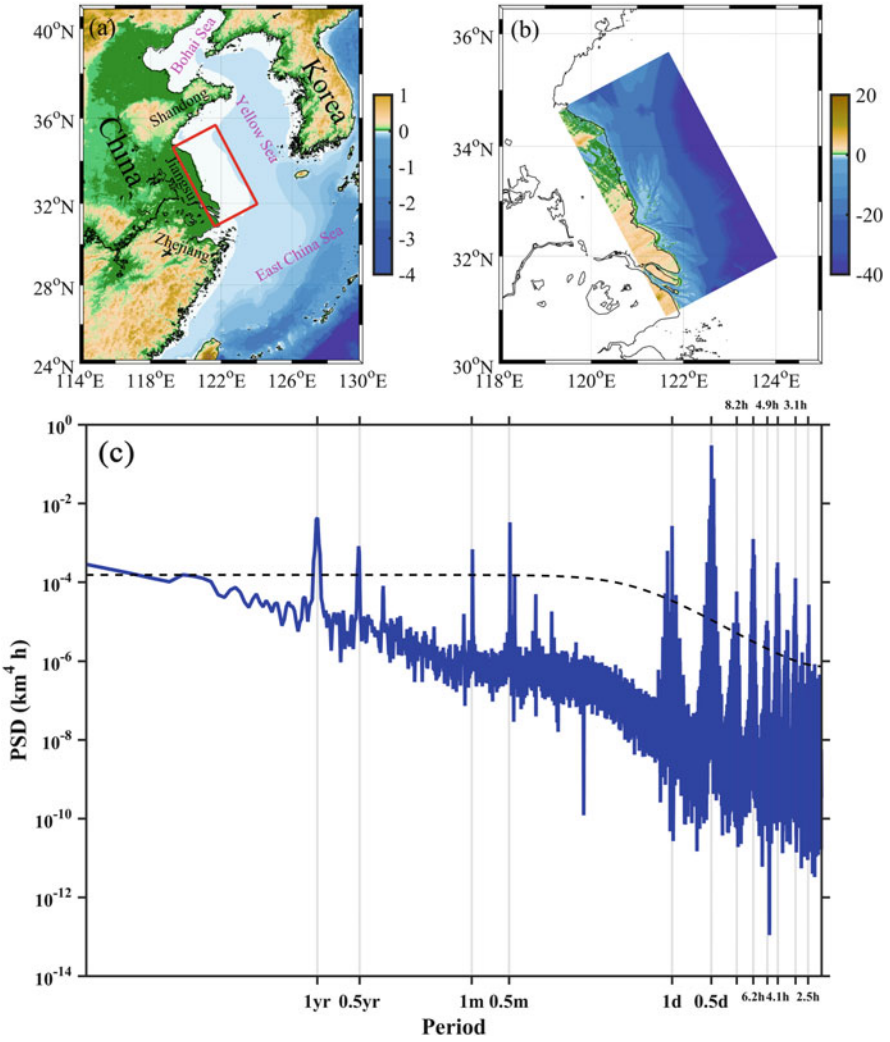

Fig. 6.6 (**a**) The location of the model domain (the red rectangle) in the East China Sea and water depth in kilometers; (**b**) expanded map of model domain with water depth in meters; and (**c**) the power spectrum of the wetland area variation. The dashed black line denotes the 95% confidence level

ocean interactions. In the example from eastern China, an Ekman current caused by the East Asian Monsoon, which blows northwesterly during the winter, induces onshore flow and, southeastward during the summer, creates offshore flow. Ekman transport (Ekman 1905) also causes long-term cycles associated with variation in Pacific gyres such as the El Niño-Southern Oscillation (ENSO) and the Pacific

Decadal Oscillation (PDO). Finally, lunar precession alters the coincidence of perigee, equinox, and lunar phase over a period of 18.6 years.

Numeric hydrodynamic models, calibrated for a particular area, have been developed and used for a variety of estuaries (e.g., Canestrelli et al. 2010; Kim 2013; Geleynse et al. 2011; Oey et al. 2007). Such models must be modified with local data to be used on another. Savenije (1992), in order to develop equations that were solvable analytically, assumed an ideal estuary, with cross-sectional area decreasing exponentially with distance from the ocean, bottom slope that was negligible, and the convergence controlled by damping of the tidal range by friction (Langbein 1963). With that assumption, tidal flow within the estuary could be modeled as a single wave at the dominant tidal frequency. Savenije et al. (2008) developed analytical solutions to model flows within such estuaries and showed the utility of such solutions to ungauged estuaries (Savenije 2015). Although not all estuaries fit the assumptions of the ideal estuary (Torres 2017), these analytic solutions have proven useful in understanding relationships related to coastal engineering, sea level rise, and ecological changes associated with salt intrusion (Savenije 2015).

Lugo et al. (1988) classified forested wetlands as riverine, fringe, and basin for both freshwater and saltwater ecosystems. They defined basin wetlands as saltwater if the basin received saline tidal water on spring tides, biweekly higher than normal tides during full and new moon. In the tropics, mangroves are present in all three of these wetland types, but TFFWs are most extensive in riverine-estuarine systems and represent the only tidal forests in temperate regions where high-salinity wetlands are dominated by marshes (Dame et al. 2000). Modeling water elevations in fringe and basin-type tidal wetlands can be accomplished with hydrodynamic models outlined above, although the basin type may also require upland hydrologic models to define freshwater inputs to the basin. Modeling TFFW water levels must involve influences of both tidal forcing and the freshwater flow (Ensign et al. 2012). This involves modeling and mapping the "tidal river" (Hoitlink and Jay 2016).

We will use the definitions of estuary and tidal river proposed by Hoitlink and Jay (2016), with the estuary upper limit at the upper point of mixed salt and fresh waters. The tidal river extends from there to the limit where tidal fluctuation of river stage is identifiable. They suggest the best method to define the upper end of the tidal river be where the variation of spring and neap tide can be identified by wavelet analysis, which will be further inland than the traditional head of the tide. These regions also fit well with the ideal estuary assumptions used by Savenije (2015) to examine ungauged estuaries. The limit of saltwater intrusion often coincides with the region where estuary width and flow are no longer decline exponentially with distance upstream. Likewise, Hackney and Avery (2015) suggest there is a distinct change in biogeochemical reactions; methanogenesis is replaced by sulfate reduction as an energy source for respiration where tidal salt concentration is 1 ppt. Horrevoets et al. (2004) combined the Savenije equations with a one-dimensional model of river hydraulics to examine influence of freshwater flow on tidal damping. They showed there is a point where tidal flow matched river flow and velocity is zero for each rate of river flow. Using a similar approach, Zhang et al. (2013) examined saltwater

intrusion in the Pearl River Delta, and Kuang et al. (2017) used the two-dimensional commercial hydraulic model MIKE 21 to examine water level changes in the Yangtze Estuary caused by river discharge (over 25,000 m^3 s^{-1}). Kuang et al. (2017) were able to estimate sea level rise into the East China Sea caused by river flood flows. Similarly, Cai et al. (2014) developed an iterative analytical model to include the residual slope due to nonlinear friction that was shown to have a substantial influence on tidal wave propagation when including the effect of river discharge when applied on Modaomen and Yangtze River estuaries. These studies demonstrate that a hydrodynamic model can be applied throughout the estuary and, similarly, a linear hydraulic model can be extended into the coastal sea to examine large river discharges.

Recent development in modeling can define tidal influence in tidal rivers that are gauged at a point upstream of the tidal reach. Estimating water budget and freshwater flow rate and timing in ungauged watersheds requires some type of hydrologic and hydraulic transport model. Several watershed-scale models have been used to predict the hydrology of inland freshwater forested wetlands (Amatya et al. 2003; Wu and Xu 2006; Wu and Johnson 2008; Dai et al. 2010, 2011; Amatya and Jha 2011; Amoah et al. 2012; Liu and Kumar 2016; Samadi et al. 2017). Recently, Golden et al. (2014) reviewed, in detail, models like SWAT, MIKESHE, HSPF, TOPMODEL, DRAINWAT, VELMA, and GBMM that are applicable for predicting wetland hydrology and assessing watershed-scale impacts of isolated wetlands. In more process-based models like MIKESHE/MIKE11 and DRAINWAT, flow in a stream/river is often modeled using the St. Venant-type continuity and momentum equations, where the upstream freshwater discharge is known and the tidal stage as the downstream boundary condition.

Depending upon the scale and nature of the problems studied, some models have also been developed specifically for estuarine tidal creeks and associated mangrove forests (Nuttle and Hemond 1988; Twilley and Chen 1998; Twilley and R-Monroy 2005; Burger et al. 2008; Blair et al. 2012; Ellis et al. 2017). However, there are only a limited number of watershed-scale models that can reliably address the hydrology, rainfall-runoff processes (Torres et al. 2004), and stream/river dynamics and their interactions in a landscape that includes the intertidal zone also affected by wind-generated waves and tidal motion and storm surge (Larson and Sato 2017).

Although basin forested wetlands cover most of the total intertidal zone in some regions of South Florida, their ecology is the least understood among mangrove types because of the complex nature of their hydrology and hydraulics. Twilley and Chen (1998) used the HYMAN model to represent the hydrology of a mangrove stand. They found runoff loss of 896 mm $year^{-1}$ and evapotranspirational loss of 967 mm $year^{-1}$ with rain input of 1097 mm $year^{-1}$ indicating subsidy from tidal inundation that occurred <5 tides per month in February to 30 tides per month in September.

Meselhe and Habib (2005) tested four different models ranging from Artificial Neural Networks (ANN), Nonparametric Regression (NPA), US Army Corps of Engineers' Gridded Surface Subsurface Hydrologic Analysis (GSSHA), HEC-HMS,

and MIKESHE to produce hydrologic predictions for a very low-gradient Vermillion, LA watershed with complex fluvial systems and tidal channels and to assess their modeling challenges. The authors concluded that while the data-driven ANN and NPR were able to reproduce the nonlinear and complex stage discharge, all three rainfall-runoff models produced similar results in predicting storm hydrographs. Rainfall resolution of 1-h duration was found adequate for simulating hydrologic processes.

Nuttle and Hemond's (1988) study showed that infiltration and ET during tidal inundation and precipitation are the dominant hydrological processes in the sediment on a marsh-wide scale. The authors also suggested that the rate and extent of advective transport by pore water drainage is controlled by marsh surface topography.

Thompson et al. (2004) linked the MIKESHE with the MIKE11 model to successfully simulate the dynamics of flooding and groundwater table for a lowland wet grassland in Southeast England. The authors pointed out the role of topographic depressions in flooding that enhanced riparian shallow water table conditions as well as evaporation from flooded ditches, conditions consistent to the TFFW. Most recently, Larson and Sato (2017) emphasized a greater need of research on processes and coupling for the complex interactions with strong feedback between the terrestrial and tidal hydrology that has to be included to improve modeling, particularly for longer time periods and larger areas in view of climate variability and change.

6.4 TFFW of the Southeastern United States: Examples from Coastal South Carolina

Although TFFWs have been studied in the Southeastern United States (Conner et al. 2007 and references therein), Coastal South Carolina (SC) is the closest equivalent to eastern China of our previous examples. Situated between 30° N and 35° N latitude, it is also in Köppens climate zone Cf with well-distributed rainfall and mild winters, as well as semidiurnal tides with a mean range of 1.5– 2 m. The primary difference is in freshwater flow and sediment supply. Since the Eastern North American continental divide is within 400 km of the Atlantic coast, rivers of the US Atlantic drainage basin are much smaller than those of eastern China.

South Carolina has three watersheds that extend to the continental divide, with rivers that form estuaries: Savannah, Santee, and Pee Dee (Fig. 6.7 inset). Tidal data has been collected for more than 50 years at three stations along the South Carolina coast: Fort Pulaski, Charleston Harbor, and Springmaid Pier. Savannah River flow is highly regulated by a series of hydroelectric reservoirs, and the lower estuary is dominated by the port of Savannah shipping channel. The Santee River flow is also regulated for hydroelectric generation as well as diverted into Charleston Harbor by an inter-basin transfer. The Pee Dee River flow is the one least impacted with only one hydroelectric reservoir in North Carolina and a shallow (<8 m) shipping channel in the lower estuary.

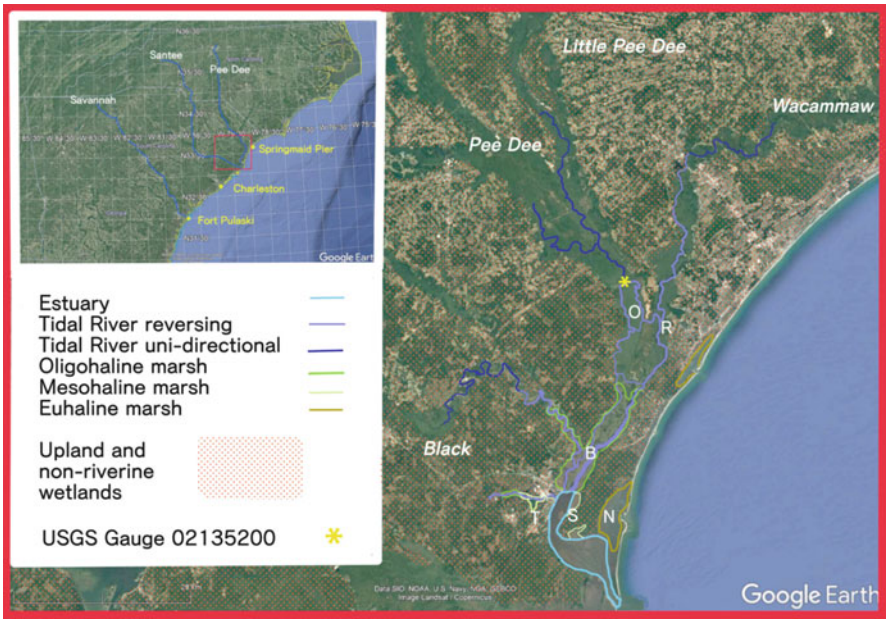

Fig. 6.7 Winyah Bay estuary and approximate locations of transitions to and within tidal rivers during average freshwater flow. Letters N, S,T,B,R, and O refer to locations of studies mentioned in text: N, North Inlet (Gardner and Bohn 1980; Wolaver et al. 1988; Morris et al. 2002); S, Strawberry Swamp (Williams et al. 2012; Jayakaran et al. 2014; Liu et al. 2017); T, B, and R, Turkey Creek, Butler Island, and Richmond Island (Noe et al. 2013, 2016; Krauss et al. 2009; Ensign et al. 2014a; Pierfelice et al. 2017); O, Bull Island (Ozalp et al. 2007)

6.4.1 Winyah Bay/Pee Dee River: Sea Level Rise in an Estuarine TFFW, Salt Impacts

The Winyah Bay estuary in Northeastern South Carolina extends from a 1-km-wide inlet (Lat. 33° 12′ 17″ N; Long. 79° 10′53″ W) for 23 km to near Georgetown, SC. The estuary is fed by four tidal rivers (Pee Dee, Little Pee Dee, Black, and Waccamaw) in the US Geologic Survey (USGS 2017) Pee Dee Hydrologic Unit (USGS Hydrologic Unit Code 0304). Within the estuary, tidal prediction is based on tidal data from the NOAA gauge at Charleston, SC (NOAA Station 8,665,530, Lat. 32° 46′ N, Long. 79° 55′ W). The Winyah Bay system has been the site with a number of studies on the TFFW (Noe et al. 2013; Krauss et al. 2009; Ensign et al. 2014a, b). Over 85% of freshwater flow into Winyah Bay originates from the Pee Dee River (Patchineelam and Kjerfve 2004), which has USGS Gauge 02135200, located 63 km from the ocean. The gauge provides continuous data on river stage, flow velocity, instantaneous discharge, and flow-averaged discharge. In addition to the rivers and estuary, the system is loosely linked to the North Inlet euhaline tidal marshes (Fig. 6.7 point N). Work at North Inlet includes early research on marsh response to sea level rise

(Wolaver et al. 1988; Morris et al. 2002; Gardner and Bohn 1980), as the area has experienced relative sea level rise for the last 6000 years (Gardner et al. 1992).

Horrevoets et al. (2004) report that within the estuary-tidal river system, a point of zero velocity will exist where the upstream tidal flow equals downstream freshwater flow. The location of that point varies with downstream flow of the river and upstream tidal flow that depends on the tidal range and the cross-sectional area of the inlet. Ensign et al. (2015) argued that sediment, C, N, and P accumulation peaked as velocity declined near the head of the tide, declined downstream within the TFFW zone, and increased again with tidal flows within the oligohaline marsh. The USGS Gauge 02135200 (USGS 2017) provides insight into variation of both the head of the tide and the point of balanced upstream and downstream flow in the Winyah Bay system. In Fig. 6.8a, the head of the tide is downstream of the gauge location for flows above approximately 730 $m^3\ s^{-1}$. In Fig. 6.8b zero velocity occurs near this point at an average daily flow of approximately 155 $m^3\ s^{-1}$. During the driest decade (2000–2009) of the 60-year record, Pee Dee median flow was 170 $m^3\ s^{-1}$, indicating the point of zero velocity was more often downstream of the gauge site, while the head of the tide was usually well upstream of the gauge.

TFFW research within the Winyah Bay system evolved from early studies of productivity on Bull Island (Ozalp et al. 2007). Bull Island (Fig. 6.7 point O) is formed by one of the several creeks connecting the tidal Pee Dee River to the tidal Waccamaw River. They found higher productivity on plots adjacent to the Pee Dee River, but productivity was lower than reported for nontidal wetlands with the same species.

The sequence of sites (Fig. 6.7 points T, B, R) from Turkey Creek (high salinity), to Butler Island (medium salinity), to Richmond Island (low salinity) has been well-studied in terms of mortality, productivity, sediment accumulation, and biogeochemistry in order to predict impact of sea level rise on TFFW.

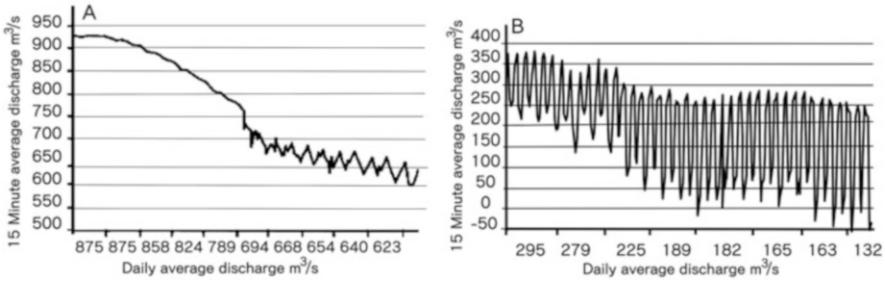

Fig. 6.8 Flow of the Pee Dee River USGS gauge 021135200. Panel **a** reflects discharge and daily mean for 10 days from 3-5-2016 to 3-15-2016. It demonstrates a constant downstream flow with no tidal fluctuation above an average flow of 730 $m^3\ s^{-1}$ with flow showing semidiurnal fluctuation below that flow rate. Panel **b** from the same site for the period 6-15-2016 to 7-5-2016 shows unidirectional flow with a semidiurnal fluctuation above flow of 155 $m^3\ s^{-1}$ and bidirectional flow when the average flow was below that value

Krauss et al. (2009) found stand basal area and growth decreases from the least saline (R) to most saline sites (T). There were also differences in soil total nitrogen, and salinity over 2 ppt resulted in forest decline. Noe et al. (2013) noted an increase in nitrogen and phosphorus mineralization R < B < T with an increase in salinity but did not see indication of sulfate reduction. Ensign et al. (2014a) found sediment accumulations decrease in the TFFW than in the adjacent mesohaline marsh at Turkey Creek (T) but did not find a significant difference in the TFFW site that had been found in a tidal river tributary to the Chesapeake Bay (Ensign et al. 2014b). They attributed the discrepancy to the location of Richmond Island (R) near a creek connected to the alluvial Pee Dee River. Noe et al. (2016) did find minimum sediment accumulations for TFFW on these sites when they examined ^{210}Pb soil profiles. Along the Waccamaw and Savannah Rivers in South Carolina, an inverse relationship between litterfall and tree woody growth and increasing salinity has been observed (Cormier et al. 2013; Pierfelice et al. 2017). Aboveground net primary productivity (litterfall plus tree woody growth) declined from 1062 g m^{-2} $year^{-1}$ in healthy freshwater swamp to 492 g m^{-2} $year^{-1}$ in moderately saline forested wetland to 79 g m^{-2} $year^{-1}$ in highly saline impacted swamp (Pierfelice et al. 2017), but there can be a great deal of variability from year to year depending upon rainfall and river discharge (Fig. 6.9).

Similar to the Turkey Creek site (T), Strawberry Swamp (S) is a small freshwater tributary of the Winyah Bay estuary within the zone of mesohaline marshes and has been subject to forest die back documented by aerial photography since 1949 (Williams et al. 2012). Presently, the area receives water with 2–10 PSU. Liu et al. (2017) found mortality of species, other than bald cypress (*Taxodium distichum* [L.] Rich.), in plots with salinity >2.6 PSU (Fig. 6.9).

Studies in the Winyah Bay estuary-tidal river system have shown that TFFW may be very susceptible to sea level rise (Figs. 6.6, 6.7, 6.8, 6.9, and 6.10). Increasing salinity associated with sea level rise will lower both biological and sedimentary input to the soil surface, suggesting they will less likely accrete material at a rate matching sea level rise. The hydraulics of the tidal rivers and hydrology of the

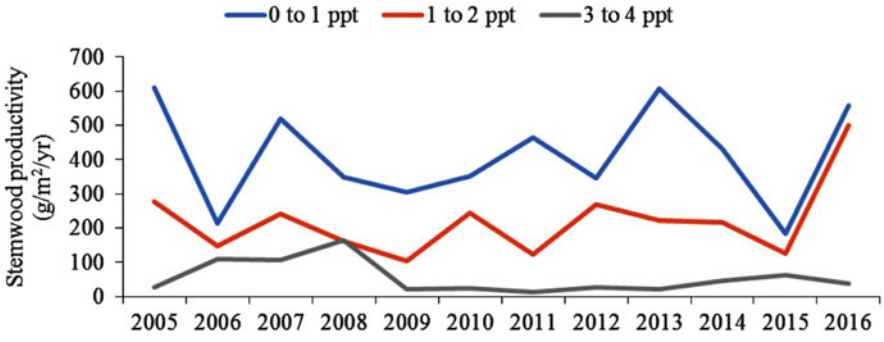

Fig. 6.9 Change in stemwood productivity along a salinity gradient in the Winyah Bay estuarine system, SC

Fig. 6.10 Strawberry Swamp, fall 2017. Liu et al. (2017) plots are in deciduous stand in center of photograph. Dead bald cypress in foreground date from 2003 to 2017

upland watersheds can also have a large impact on potential accretion. In the Winyah Bay system, the head of the tide moved over 35 km downstream with a moderately high freshwater flow.

6.4.2 Charleston–East Cooper River: Sea Level Rise and TFFW Impact of Higher Freshwater Tides

In contrast to the Pee Dee River system, the Santee system and the Charleston harbor drainage have been highly impacted by human intervention. By exploiting the location of a prominent marine terrace (Cooke 1936), the Santee River could be dammed to produce a large upstream reservoir (Lake Marion) and diverted to create another large reservoir (Lake Moultrie). From Lake Moultrie another short canal connected to the upper west Cooper River creates over 20 m of head for hydroelectric generation. Flow from the Santee was diverted into this station in 1947. Siltation and high dredging costs in the Charleston Harbor required digging another canal from Lake Moultrie back to the Santee with much less efficient hydroelectric generation in 1987. The need to maintain a freshwater supply to industrial development during the intervening 40 years required that a flow of 142 m^3 s^{-1} be

maintained in the West Branch of the Cooper River. Due to this, upper reaches of the East Branch of the Cooper River have a freshwater tide with a mean range of 1.28 m (Czwartacki 2013) at the upland freshwater forested wetland watersheds maintained by the USDA Forest Service Santee Experimental Forest (SEF).

Earlier modeling studies using the MIKE SHE model (Dai et al. 2010, 2011) for first- and second-order watersheds successfully captured both daily water table and streamflow dynamics, while the SWAT model (Amatya and Jha 2011) captured streamflow dynamics for adjacent third-order forested wetland watersheds at the SEF site on the South Carolina Atlantic coastal plain. These freshwater wetland sites are headwaters of the tidally influenced Huger Creek with an area of 235 km^2 that discharges to the East Branch of the Cooper River draining into the Charleston Harbor/estuary. Based on a limited shallow groundwater table behavior pilot study on the intertidal riparian forest buffer affected by diurnal tidal fluctuation (Fig. 6.12), Czwartacki (2013) suggested the tidal creek functions as a freshwater reservoir to the adjacent riparian wetland through the daily tide cycle. The results demonstrate the need to assess nontidal and tidally influenced wetlands separately when considering their hydrology and functions in the landscape, which is fundamental to understanding how sea level rise will affect habitat quality, nutrient exchange, and sediment transport to the estuary. Although Larson and Sato (2017) recently reviewed some complex equations to model short and long waves, nearshore circulation, and sediment transport for these systems, as a current state of the art, the MIKESHE-DNDC model linked with MIKE11 using high-resolution geospatial and other ecohydrological data (as shown below) has been proposed as a tool, after a proper validation, to assess the fate of upstream freshwater outflow and material from this intertidal site (Fig. 6.11) during its transport downstream to tidal creek/estuaries that is further complicated by changing land use and climate change.

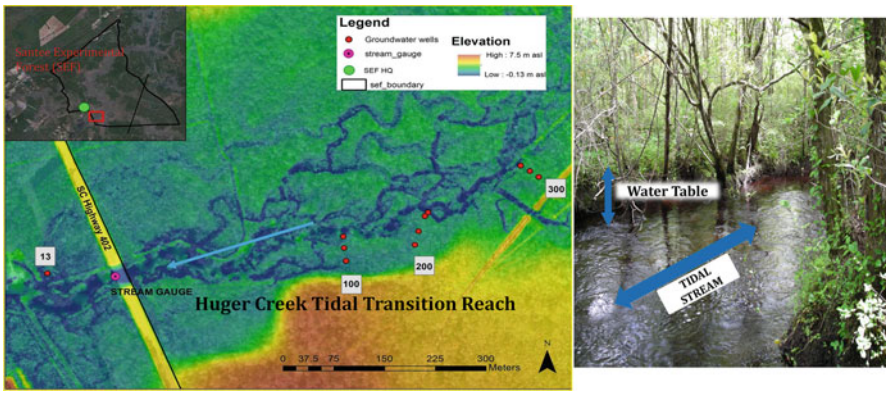

Fig. 6.11 Huger Creek site layout of monitoring infrastructure (left); Huger Creek stream channel at SC Highway 402 Bridge (top middle); hummock and hollow typical micro-topography (bottom middle); tidal stream and riparian freshwater forested wetland (top-right); and mean water table elevation trend from downstream tidal to upstream freshwater stream bank (bottom-right)

6.4.2.1 Geospatial Modeling of Climate Change Tidal Ranges on the East Copper River Region

Using a global geospatial framework, Vörösmarty et al. (2010) demonstrated that the pandemic impacts on both human water security (HWS) and freshwater biodiversity (BD) were highly coherent, although not identical. They scaled the HWS and BD of the Atlantic and Gulf coasts of the United States as high to very high. The incident threats arose from the spatial coincidence of multiple themes, such as water disturbance, water resources development, biotic, and pollution factors that includes soil salinity (Vörösmarty et al. 2010). Freshwater systems, including coastal ones, are directly vulnerable to human activities (e.g., widespread land cover change, urban sprawl, and engineering designs like reservoirs, irrigation, and inter-basin water transfers) (Meybeck 2003; Karl et al. 2009; WWAP 2009) and are expected to be further impacted by anthropogenic climate change (e.g., tidal surge and subsequent soil salinity intensification) (Karl et al. 2009). TFFWs are directly impacted by sea level rise and climate change (Baldwin et al. 2009). The findings by Kirwan et al. (2010) that coastal marshes with low suspended sediment concentration (SSC) and low tidal range would be submerged at smaller sea level rise rates than the marshes with high SSC and high tidal ranges would potentially be applicable to the intertidal TFFW as well. Enormous quantities of water flow in and out of southeastern Atlantic coast wetlands twice a day and at higher tidal stages a minimum of two times a lunar month, which create alternately flooded and non-flooded conditions throughout these wetlands (Savenije 2005; Baldwin et al. 2009).

Biodiversity in the southeastern Atlantic coastal plain would be immensely affected when TFFWs are inundated with saline water, and, hence, prior spatial knowledge would help in its mitigation decision support. Long duration water intrusion, due to increase in height of the low amplitude tides that inundates TFFW twice every day, would convert those stands to freshwater marsh (some of these factors, particularly vegetation, will be discussed in Sect. 6.4.3). Well-drained soil in TFFW may quickly drain the water, and thus impact is anticipated to be less to the plant roots and vice versa. Najjar et al. (2000), through their study on potential impacts of climate change on the mid-Atlantic coastal region, concluded that tidal surges of more than 2 m above the present mean sea level could be the future norm.

The lower South Carolina coastal plain near Charleston (Fig. 6.12) was delineated using ArcSWAT (Soil & Water Assessment Tool, http://swat.tamu.edu/) using the Cooper River confluence of the East and West branch of the Copper as the exit point. The change in elevation on the river ranges from 0 MSL at Charleston Harbor to approximately 1.5 m above MSL at the upstream point (USACOE 2017). According to Kana et al. (1984), the tidal range increases considerably from north to south along South Carolina's shoreline, from approximately 1.7 m at the northern border to 2.7 m at the southern border. Due to the flatness of the study area, soils in this watershed range from mostly poorly drained with few well drained, possibly enhancing the impact of tidal inundation on TFFW. It is to be noted that the yellow line in Fig. 6.12 represents South Carolina Division of Natural Resources' (SC-DNR) delineation of the saltwater/freshwater interface, approximately limit of 1 ppt salinity in tidal creeks.

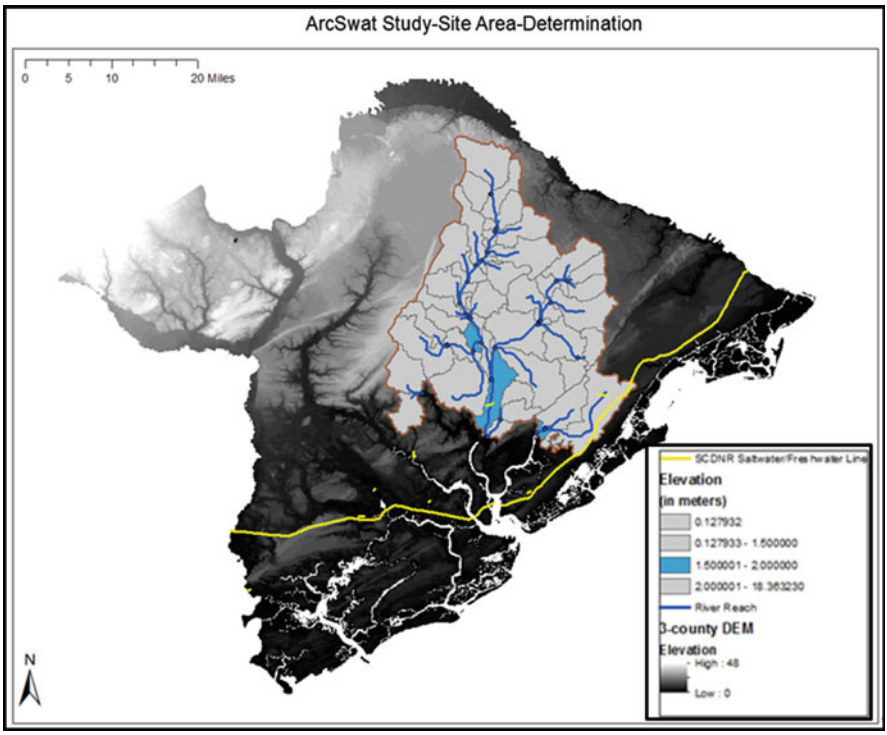

Fig. 6.12 Area used for studying climate change indicated tidal range impact on TFFW biodiversity in South Carolina

6.4.2.2 Discussion of Modeling Results

Figure 6.13a depicts the area that will be inundated with an assumed 2 m high tide as the elevation of the spatial locations is $\leq$2 m above MSL. Figure 6.13b shows the four gSSURGO-based soil characteristic rasters (drainage, available water storage (AWS), soil hydrologic group, and texture) that were classified and reclassified to show the potential area that would be affected due to saltwater intrusion according to their ability to drain saline/brackish water after tidal surge. If the tidal inundated area does not drain quickly, creating saturated soil for long periods, it will likely affect the flora and subsequent ecosystems of the TFFW. Figure 6.13c shows impacted spatial locations and classified land cover (including vegetation) of the area, which was developed with both elevation and soil characteristics integration. The affected land cover classes are Huger Park (estuarine marine wetland), HC201 (freshwater emergent wetland), HC101 (freshwater forested shrub), and swamp (nomenclature based on the National Wetland Inventory (NWI) classification scheme). Figure 6.13c also shows the selected sample point locations for ground-truthing and subsequent accuracy assessment. Table 6.1 shows the TFFW land cover class distribution that

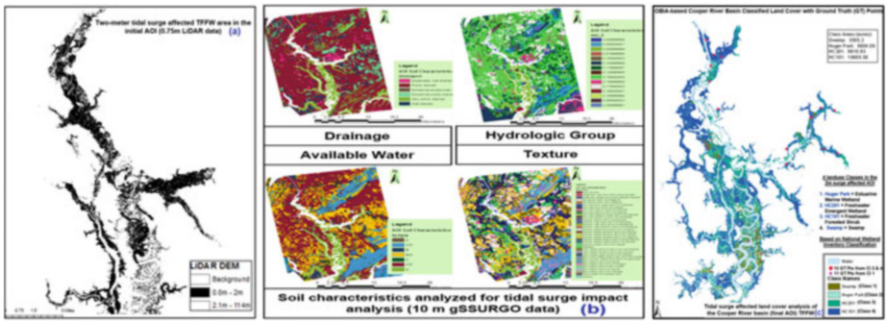

Fig. 6.13 Results (shown in a workflow basis) of saline water inundation analysis using (**a**) DEM (0.75 m), (**b**) gSSURGO (10 m), and (**c**) NAIP (1 m) imagery OBIA classification-based decision support

Table 6.1 Land cover distribution of the probable 2 m tidal surge affected TFW in Charleston, SC area

Land cover class		Land cover class	
NWI classification (https://www.fws.gov/wetlands/data/mapper.html)	Area (ha)	OBIA image segmentation	Area (ha)
Estuarine marine wetland	1019	Estuarine marine wetland	2794
Freshwater emergent wetland	4955	Freshwater emergent wetland	3485
Freshwater forested shrub	9390	Freshwater forested shrub	7954
		Swamp	1418

will be inundated and affected due to probable 2 m tidal surges. OBIA-based land cover classification results (2015) differed from the NWI (2011) classification results, and this was attributed to the temporal difference of the image analysis. With a total of 13 ground-truthed samples (Fig. 6.12c) selected from freshwater emergent wetland (8) and freshwater forested shrub (5) classes, a 100% overall accuracy was obtained with land cover classification, and all locations were ascertained with zero salinity. The swamp (freshwater herbaceous wetland) and the estuarine marine wetland classes were visually verified with NWI data layer (Table 6.1), and 100% accuracy of land use class was obtained with randomly chosen 11 sample points (Fig. 6.13c).

6.4.2.3 Conclusions of Modeling Efforts

Ultra-high-resolution data like LiDAR are very data-intensive and need advanced knowledge and high-end processing computers to obtain DEM and other intermediary products like nDSM. However, it is very useful as the elevation information obtained from the LiDAR data is accurate and up-to-date. High-resolution (10 m)

gSSURGO data available in the United States provides a better perspective of decision-making on such tidal-based TFFW effect analyses. gSSURGO data contains many soil hydraulic characteristics (attributes) that enhance analyses. However, this model uses a static LIDAR-based estimation of surge elevations, similar to the method of Craft et al. (2009). Surge estimates made with hydrodynamic models such as SLOSH (Jelesnianski et al. 1992) or CEST (Xiao et al. 2006) allow estimation of surge attenuation due to friction and are likely to produce more accurate estimates of tidal elevation in the upper reaches of the estuary.

6.4.3 Review of TFFW in the Southeastern United States

TFFWs in general are defined as occurring at salinities below 0.5 ppt (Odum et al. 1984), with an important transition occurring as mean salinity levels exceed 2 ppt (Hackney et al. 2007). These forests are flooded and drained regularly by freshwater overflow attributed to local high tides, and they are also prone to saltwater influx during low river discharge (as occurs in drought years) or high storm tides (usually during hurricanes) and by sea level rise and climate change (Baldwin et al. 2009). Tide patterns vary across the range of tidal forests from diurnal, semidiurnal, or mixed and are of different amplitudes and range depending upon the location (Doyle et al. 2007). Hydrology within these forests can be difficult to interpret because of river discharge, tidal stage and bidirectional flow, local precipitation, evapotranspiration, groundwater, and prevailing winds (Anderson and Lockaby 2011). River discharge and tidal stage vary on a seasonal basis and have potential implications for wetland saltwater intrusion. The geomorphology of the estuary and coast determines the amplitude, duration, and velocity of ebb and flow stages, resulting in forests subject to regular flooding from <1 m once a day in the western Gulf of Mexico (Apalachicola Bay in Florida to southern tip of Texas) to between 2 and 3 m twice a day on the Atlantic coast (southern North Carolina to Northeast Florida) (Officer 1976; Savenije 2005; Doyle et al. 2007; Wolanski 2007; Baldwin et al. 2009). Information regarding tidal freshwater swamps is generally sparse in the literature, but there has been an increased interest in these areas since the publication of the book *Ecology of Tidal Freshwater Forested Wetlands of the Southeastern United States* (Conner et al. 2007) and also the increased coastal urbanization encroaching these sensitive systems.

6.4.3.1 Composition

Canopy tree richness varies from region to region (see, e.g., Rheinhardt 1992; Light et al. 2007; Duberstein and Kitchens 2007) depending on hydrology, geomorphology, soils, and salinity (Sharitz and Mitsch 1993; Brinson 1995; Lockaby and Walbridge 1998; Mitsch and Gosselink 2000), but bald cypress (*Taxodium distichum* [L.] Rich.), water tupelo (*Nyssa aquatica* L.), swamp tupelo (*Nyssa biflora* Walter),

red maple (*Acer rubrum* L.), and ash (*Fraxinus* spp.) are the tree species most commonly associated with TFFW of the Southern United States. These trees are sensitive to saltwater intrusion, with bald cypress generally being the most salt tolerant, although its growth is reduced considerably at mean annual salinity concentrations above 2 ppt (Hackney et al. 2007; Krauss et al. 2009). Understory trees, shrub, and herb layers are generally sparse and low in diversity because of dense canopy and frequent flooding in the upper reaches of the river. However, as salinity levels increase, tree canopy decreases, resulting in more extensive and species-rich subcanopies and herbaceous layers (Mitsch et al. 2009).

There are areas on the Atlantic coast (primarily North Carolina) and Gulf Coast (Mississippi) where Atlantic white cedar (*Chamaecyparis thyoides* [L.] Britton, Sterns & Poggenb.) occurs in areas subjected to wind-driven tides (Keeland and McCoy 2007), and the trees are concentrated on hummocks (Laderman 1989). Atlantic white cedar is not typically tolerant of salinity (Moore and Carter 1987), and mature tree vigor is impacted when storm surges bring brackish waters into these forests (Keeland and McCoy 2007).

In the Big Bend area of Florida, islands of freshwater forest (isolated remnants of a formerly continuous forest that is retreating landward) are found. These islands are dominated by cabbage palmetto (*Sabal palmetto* [Walt.] Lodd ex Schult) and southern red cedar (*Juniperus virginiana var. silicicola* Small) that occur on elevated limestone substrate surrounded by salt marsh (Kurz and Wagner 1957; Williams et al. 1999a, b, 2007; DeSantis et al. 2007; Geselbracht et al. 2011). *Cabbage palmetto*, which is one of the most salt-tolerant trees in the Southeastern United States (Perry and Williams 1996), is the sole tree species on the most saline islands.

6.4.3.2 Hydroperiods

A wetland's hydroperiod (flood frequency, duration, depth, and timing) determines which species will germinate, become established, and persist in a given wetland area. Seeds of bald cypress and water tupelo, two of the most flood-tolerant trees found in tidal freshwater forested wetlands (Hook 1984), do not germinate in continuously flooded soils (DuBarry 1963). Increased flooding and extended waterlogging result in decreased photosynthesis (McLeod et al. 1996) and growth (Pezeshki et al. 1987; Young et al. 1995), with eventual mortality to those species that are less flood tolerant (Harms et al. 1980).

6.4.3.3 Salinity

Rising sea level leads not only to increases in hydroperiod with possible increased runoff but increased salinity as well. Bald cypress trees seem to be the most salt-tolerant trees in TFFW, with Louisiana genotypes more tolerant than genotypes from other southeastern states (Conner and Inabinette 2005). Successful bald cypress regeneration and establishment along the Northeast Cape Fear River only occurred

in areas with interstitial salinities less than 2 ppt (Fleckenstein 2007). When interstitial salinity becomes too high for even bald cypress to survive, TFFWs undergo a state change to oligohaline marsh (Effler et al. 2007; Fleckenstein 2007). When tidal flooding frequency exceeds 10–20 days per year, natural seedling emergence and survival of cabbage palm trees in Florida's tidally influenced hydric hammocks decline drastically (Williams et al. 2007).

The establishment of species zonation along salinity gradients is thought to result from pulses of saltwater, rather than slow gradual change (Duberstein 2011). Salinity pulses can be a result of storm surges that occur frequently enough to have important effects on tidal freshwater forested wetlands (Light et al. 2007) or from extended drought conditions. Tree mortality rates of roughly 10% per year occurred for three consecutive years following a saltwater intrusion event into the swamps immediately adjacent to Maurepas Lake (Louisiana), though bald cypress trees were affected less (Shaffer et al. 2003). Brinson et al. (1985) and Baldwin (2007) agree that pulses such as these shape the structure and productivity of tidal freshwater swamps more than long-term averages.

6.4.3.4 Productivity

Growth of bald cypress is reduced considerably at mean annual salinity concentrations above 2 ppt. Above this level, basal area, forest height, and basal increment are not sufficient to allow persistence of any forested wetland tree species into the future. Studies on the lower Cape Fear (NC), Waccamaw River (SC), Savannah River (GA), and southeastern Louisiana found that tidal bald cypress swamps are all actively converting to marsh (Hackney et al. 2007; Krauss et al. 2009; Shaffer et al. 2009). In Louisiana, bald cypress sites that are at or above the 2 ppt salinity threshold appear to be converting to marsh at a slower rate, but these sites are definitely deteriorating (Krauss et al. 2009). With increasing salinity, tree growth is diminished, and there is increased mortality of tidal swamp trees. While mean annual site salinity ranged from 0.1 to 3.4 ppt, sites with salinity concentrations of 1.3 ppt or greater supported a basal area of less than 40 $m^2\ ha^{-1}$. Where salinity was 0.7 ppt, basal area was as high as 87 $m^2\ ha^{-1}$ (Krauss et al. 2009). Eventually, these forests become marsh with standing snags, earning these areas the name "ghost forests."

6.5 Summary and Future Prospects

Although study of tidal forested wetlands has been relatively recent, the potential to increase our understanding of these wetlands has been greatly increased by development of a number of advances in other sciences. Although the strong role of the phases of the moon on tidal stage has been recognized for over 2000 years, our ability to measure and predict tidal motions over the globe only occurred following

the development of satellite altimetry with the strong feedback between satellite altimetry and hydrodynamic modeling. We can now measure global decadal average sea level rise with errors on the order of 0.4 mm $year^{-1}$ although annual estimates vary by well over 1 mm $year^{-1}$ (Albain et al. 2017).

As demonstrated by the East China Sea wetland example, robust hydrodynamic modeling must be combined with remote sensing to determine the tidal stage at the time each scene is collected to produce meaningful environmental information about tidal wetland status. Such methods are likely to also be highly beneficial to our studies of changes to TFFW and mangrove ecosystems.

A great deal of our present knowledge of TFFW comes from plot research. Most hydrologic understanding comes from empirical measurements made on plots that were chosen due to vegetational characteristics. Modern hydrodynamic, hydraulic, and hydrologic modeling may be capable of estimating all the variation in TFFW wetlands caused by interactions of rainfall, upland runoff, river flooding, and tidal fluctuations. Understanding these hydrologic factors may put our previous physiological and biogeochemical findings into a framework that would allow prediction of the factors that are important to productivity of TFFW. Such understanding may be critical as Woodruff et al. (2013) suggest that uncertainty in changes in predicted number tropical cyclones, probable increase in cyclone intensity, and sea level rise will combine to impact coastal regions in ways that haven't occurred since the end of the ice age.

Acknowledgments We thank anonymous reviewers for their thoughtful comments and suggestions, which improved the manuscript. Part of the research included in this review was funded by the US Geological Survey, Climate and Land Use Change Research and Development Program, and also supported in part by the National Institute of Food and Agriculture, US Department of Agriculture, under award number SCZ-1700531. Technical Contribution No. 6654 of the Clemson University Experiment Station. Thanks are also due to USDA Forest Service Southern Research Station and 10th INTECOL Conference for their support of the INTECOL special session followed by initiating this chapter.

References

Albain M, Legais JF, Prandi P, Marcos M, Fenoglio-Marc L, Dieng HB, Benevniste J, Cazenve A (2017) Satellite altimetry based sea level at global and regional scales. Surv Geophys 38:7–31

Alesheikh AA, Ghorbanali A, Nouri N (2007) Coastline change detection using remote sensing. Int J Environ Sci Technol 4(1):61–66

Algoni DM (2002) Present state and future of the world's mangrove forests. Environ Conserv 29:331–349. https://doi.org/10.1017/S0376892902000231

Amatya DM, Jha MK (2011) Evaluating SWAT model for a low gradient forested watershed in coastal South Carolina. Trans ASABE 54(6):2151–2163

Amatya DM, Chescheir GM, Fernandez GP, Skaggs RW, Birgand F, Gilliam JW (2003) Lumped parameter models for predicting nitrogen transport in lower coastal plain watersheds. Report No. 347, Water Resources Research Institute of University of the North Carolina, Raleigh, NC, p 118

Amoah J, Amatya DM, Nnaji S (2012) Quantifying watershed depression storage: determination and application in a hydrologic model. Hydrol Process 27(17):2401–2413. https://doi.org/10.1002/hyp.9364

Anderson CJ, Lockaby BG (2011) Forested wetland communities as indicators of tidal influence along the Apalachicola River, Florida, USA. Wetlands 31:895–906

Baldwin AH (2007) Vegetation and seed bank studies of salt-pulsed swamps of the Nanticoke River, Chesapeake Bay. In: Conner WH, Doyle TW, Krauss KW (eds) Ecology of tidal freshwater forested wetlands of the Southeastern United States. Springer, Dordrecht, pp 139–160

Baldwin AH, Barendregt A, Whigham DF (2009) Tidal freshwater wetlands—an introduction to the ecosystem. In: Barendregt A, Whigham DF, Baldwin AH (eds) Tidal freshwater wetlands. Backhuys Publishers, Leiden, pp 1–10

Barbier EB, Hacker SD, Kennedy C, Koch EW, Stier AC, Silliman BR (2011) The value of estuarine and coastal ecosystem services. Ecol Monogr 81:169–193

Barendregt A, Whigham DF, Baldwin AH (2009) Tidal freshwater wetlands. Backhuys Publishers, Leiden

Batzer DP, Baldwin AH (2012) Wetland habitats of North America: ecology and conservation concerns. University of California Press, Berkeley, CA

Blair AC, Sanger DM, White DL, Holland AF, Vandiver LA, Bowker C, White S (2012) Quantifying and simulating stormwater runoff in watersheds. Hydrol Process 28(3):559–569. https://doi.org/10.1002/hyp.9616

Blumberg AF, Mellor GL (1987) A description of a three-dimensional coastal ocean circulation model. In: Heaps N (ed) Three-dimensional coastal ocean models, vol 4. American Geophysical Union, Washington, DC

Brinson MM (1995) The HGM approach explained. Natl Wetl Newsl 17:7–13

Brinson MM, Bradshaw HD, Jones MN (1985) Transitions in forested wetlands along gradients of salinity and hydroperiod. J Elisha Mitchell Sci Soc 101:76–94

Burger U, Rivera-Monroy VH, Doyle TW, Dahdous-Guebas F, Duke NEC, Fontalzo-Heraldo ML, Hildenbrandt H, Koedam N, Mehlig U, Piou C, Twilley RR (2008) Advances and limitations of individual-based models to analyze and predict dynamics of mangrove forests: a review. Aquat Bot 89:260–274

Cai H, Savenije HHG, Toffolon M (2014) Linking the river to the estuary: influence of river discharge on tidal damping. Hydrol Earth Syst Sci 18:287–304. https://doi.org/10.5194/hess-18-287-2014

Canestrelli A, Fagherazzi S, Defina A, Lanzoni S (2010) Tidal hydrodynamics and erosional power in the Fly River delta, Papua New Guinea. J Geophys Res 115:F04033. https://doi.org/10.1029/2009JF001355

Carter RWG (1990) Coastal environments: an introduction to the physical, ecological and cultural systems of coastlines. Academic, London

Chen JY, Zhu HF, Dong YF, Sun JM (1985) Development of the Changjiang estuary and its submerged delta. Cont Shelf Res 4(1/2):47–56

Conner WH, Inabinette LW (2005) Identification of salt tolerant bald cypress (*Taxodium distichum* (L.) Rich) for planting in coastal areas. New For 29:305–312

Conner WH, Doyle TW, Krauss KW (eds) (2007) Ecology of tidal freshwater forested wetlands of the Southeastern United States. Springer, Dorcrecht

Cooke CQ (1936) Geology of the coastal plain of South Carolina. Bulletin 867. US Geological Survey, U.S. Government Printing Office, Washington, DC

Cormier N, Krauss KW, Conner WH (2013) Periodicity in stem growth and litterfall in tidal freshwater forested wetlands: influence of salinity and drought on nitrogen recycling. Estuar Coasts 36(3):533–546

Craft C, Clough J, Ehman J, Joye S, Park R, Pennings S, Guo H, Machmuller M (2009) Forecasting the effects of accelerated sea-level rise on tidal marsh ecosystem services. Front Ecol Environ 7(2):73–78. https://doi.org/10.1890/070219

Czwartacki BJ (2013) Time and tide: understanding the water dynamics in a tidal freshwater forested wetland. M.S. thesis, Graduate School, College of Charleston, Charleston, SC, p 129

Dai Z, Li C, Trettin CC, Sun G, Amatya DM, Li H (2010) Bi-criteria evaluation of the MIKE SHE model for a forested watershed on the South Carolina coastal plain. Hydrol Earth Syst Sci 14:1033–1046

Dai Z, Trettin CC, Li C, Li H, Sun G, Amatya DM (2011) Effect of assessment scale on spatial and temporal variations in CH_4, CO_2, and N_2O fluxes in a forested wetland. Water Air Soil Pollut 223(1):253–265. https://doi.org/10.1007/s11270-011-0855-0

Dame R, Alber M, Allen D, Mallin M, Montague C, Lewitus A, Chalmers A, Gardner LR, Gilman C, Kjerfve B, Pickney J, Smith N (2000) Estuaries of the South Atlantic Coast of North America: their geographical structure. Estuaries 23:793–819

Darwin GH (1901) The tides. John Murray, London, p 346

Day RH, Williams TM, Swarzenski CM (2007) Hydrology of tidal freshwater forested wetlands of the Southeastern United States. In: Conner WH, Doyle TW, Krauss KW (eds) Ecology of tidal freshwater forested wetlands of the Southeastern United States. Springer, Dordrecht, pp 29–63

Dellepiane S, De Laurentiis R, Giordano F (2004) Coastline extraction from SAR images and a method for the evaluation of the coastline precision. Pattern Recogn Lett 25(13):1461–1470

DeSantis LR, Bhotika S, Williams K, Putz FE (2007) Sea-level rise and drought interactions accelerate forest decline on the Gulf Coast of Florida, USA. Glob Chang Biol 13:2349–2360

Diefenderfer HL, Coleman AM, Borde AB, Dinks IA (2008) Hydraulic geometry and microtopography if tidal forested freshwater wetlands and implications for restoration. Ecohydrol Hydrobiol 8:339–361. https://doi.org/10.2478/v10104-009-0027-7

Doodson AT (1921) The harmonic development of the tide-generating potential. Proc R Soc Lond A 100:305–329. https://doi.org/10.1098/rspa.1921.0088. http://rspa.royalsocietypublishing.org/. Accessed 18 Apr 2018

Doyle TW, Conner WH, Ratard M, Inabinette LW (2007) Assessing the impact of tidal flooding and salinity on long-term growth of bald cypress under changing climate and riverflow. In: Conner WH, Doyle TW, Krauss KW (eds) Ecology of tidal freshwater forested wetlands of the Southeastern United States. Springer, Dordrecht, pp 411–445

DuBarry AP Jr (1963) Germination of bottomland tree seed while immersed in water. J For 61:225–226

Duberstein JA (2011) Composition and ecophysiological proficiency of tidal freshwater forested wetlands: investigating basin, landscape, and microtopographical scales. Ph.D. thesis, Clemson University, Clemson, SC

Duberstein J, Kitchens WM (2007) Community composition of select areas of freshwater tidal forest along the Savannah River. In: Conner WH, Doyle TW, Krauss KW (eds) Ecology of tidal freshwater forested wetlands of the Southeastern United States. Springer, New York, pp 321–348

Effler RS, Shaffer GP, Hoeppner SS, Goyer RA (2007) Ecology of the Maurepas Swamp: effects of salinity, nutrients, and insect defoliation. In: Conner WH, Doyle TW, Krauss KW (eds) Ecology of tidal freshwater forested wetlands of the Southeastern United States. Springer, Dordrecht, pp 349–384

Egbert GD, Erofeeva SY, Ray RD (2010) Assimilation of altimetry data for nonlinear shallow-water tides: quarter-diurnal tides of the Northwest European Shelf. Cont Shelf Res 30(6):668–679. https://doi.org/10.1016/j.csr.2009.10.011

Ekman VW (1905) On the influence of the earth's rotation on ocean currents (Arkiv för Matematik Astronomi och Fysik band 2 no. 11 Upsalla Sweden Almqvist and Wiksells Boktryckeri-A.-B)

Ekman M (1993) A concise history of the theory of tides, precession–nutation and polar motion (from antiquity to 1950). Surv Geophys 14:585–617

Ellis K, Callahan TJ, Greenfield DI, Sanger D, Robinson J, Jones M (2017) Measuring and modeling flow rates in tidal creeks: case study from the central coast of South Carolina. J S Carol Water Res 4(1):21–39

Ensign SH, Noe GB, Hupp CR, Fagherazzi S (2012) A meeting of the waters: interdisciplinary challenges and opportunities in tidal rivers. EOS Trans Am Geophys Union 93(45):455–456

Ensign SH, Hupp CR, Noe GB, Krauss KW, Stagg CL (2014a) Sediment accretion in tidal freshwater forests and oligohaline marshes of the Waccamaw and Savannah Rivers, USA. Estuar Coasts 37(5):1107–1119

Ensign SH, Noe GB, Hupp CR (2014b) Linking channel hydrology with riparian wetland accretion in tidal rivers. J Geophys Res Earth Surf 119:28–44. https://doi.org/10.1002/2013JF002737

Ensign SH, Noe GB, Hupp CR, Skalak KJ (2015) Head-of-tide bottleneck of particulate material transport from watersheds to estuaries. Geophys Res Lett 42. https://doi.org/10.1002/2015GL066830

Fang G, Wang Y, Wei Z, Choi BH, Wang X, Wang J (2004) Empirical cotidal charts of the Bohai, Yellow, and East China Seas from 10 years of TOPEX/Poseidon altimetry. J Geophys Res Atmos 109(C11):227–251. https://doi.org/10.1029/2004JC002484

Fleckenstein EL (2007) The influence of salinity on the germination and distribution of *Taxodium distichum* (L.) Rich. bald cypress, along the Northeast Cape Fear River. MSc thesis, University of North Carolina Wilmington, Wilmington, NC

Gao S (2009) Modeling the preservation potential of tidal flat sedimentary records, Jiangsu coast eastern China. Cont Shelf Res 29:192–1936

Gardner LR, Bohn M (1980) Geomorphic and hydraulic evolution of tidal creeks on a subsiding beach ridge plain, North Inlet, S.C. Mar Geol 34: M91–M97

Gardner LR, Smith BR, Michener WK (1992) Soil evolution along a forest salt-marsh transect under a regime of slowly rising sea-level, Southeastern United States. Geoderma 55:141–157

Geleynse N, Storms JE, Walstra DJR, Jagers HA, Wang ZB, Stive MJ (2011) Controls on river delta formation; insights from numerical modelling. Earth Planet Sci Lett 302(1):217–226

Gens R (2010) Remote sensing of coastlines: detection, extraction and monitoring. Int J Remote Sens 31(7):819–1836

Geselbracht L, Freeman K, Kelly E, Gordon DR, Putz FE (2011) Retrospective and prospective model simulations of sea level rise impacts on Gulf of Mexico coastal marshes and forests in Waccasassa Bay, Florida. Clim Chang 107:35–57

Golden HE, Lane CR, Amatya D, Bandilla K, Raanan-Kiperwas H, Ssegane H (2014) Modeling watershed-scale hydrologic connections between geographically isolated wetlands and surface water systems. J Environ Model Softw 53:190–206

Hackney CT, Avery CB (2015) Tidal wetland community response to varying levels of flooding by saline water. Wetlands 35:227–236. https://doi.org/10.1007/s13157-014-0597-z

Hackney CT, Avery GB, Leonard LA, Posey M, Alphin T (2007) Biological, chemical, and physical characteristics of tidal freshwater swamp forests of the Lower Cape Fear River/Estuary, North Carolina. In: Conner WH, Doyle TW, Krauss KW (eds) Ecology of tidal freshwater forested wetlands of the Southeastern United States. Springer, Dordrecht, pp 183–221

Halpern BS, Walbridge S, Selkoe KA, Kappel CV, Micheli F, D'Agrosa CD, Bruno JF et al (2008) A global map of human impact on marine ecosystems. Science 319:948–952

Harms WR, Schreuder HT, Hook DD, Brown CL, Shropshire FW (1980) The effects of flooding on the swamp forest in Lake Ocklawaha, Florida. Ecology 61:1412–1421

Hoitlink AJF, Jay DA (2016) Tidal river dynamics: implications for deltas. Rev Geophys 54:240–272. https://doi.org/10.1002/2015RG000507

Hook DD (1984) Waterlogging tolerance of lowland tree species of the south. South J Appl For 8:136–149

Horrevoets AC, Savenije HHG, Schuurman JN, Graas S (2004) The influence of river discharge on tidal damping in alluvial estuaries. J Hydrol 294:213–228

Jayakaran AD, Williams TM, Conner WH, Hitchcock DR, Song B, Chow AT, Smith EM (2014) Monitoring water quality changes in a forested freshwater wetland threatened by salinity. In: Proceedings of the 2014 South Carolina Water Resources Conference, held October 15–16, 2014 at the Columbia Metropolitan Convention Center

Jelesnianski CP, Chen J, Shaffer WA (1992) SLOSH: sea, lake and overland surges from hurricanes. National Oceanic and Atmospheric Administration, Washington, DC

Jordi A, Wang DP (2012) sbPOM: a parallel implementation of Princeton Ocean Model. Environ Model Softw 38:59–61. https://doi.org/10.1016/j.envsoft.2012.05.013

Kana TW, Siah SJ, Williams ML, Sexton WJ (1984) Analysis of historical erosion rates and prediction of future shoreline positions, Myrtle Beach, South Carolina. Summary Rept. for South Carolina Coastal Council and City of Myrtle Beach, RPI, Columbia, S.C., p 113

Karl TR, Melillo JM, Peterson TC (eds) (2009) Global climate change impacts in the United States. Cambridge University Press, New York

Keeland BD, McCoy JW (2007) Plant community composition of a tidally influenced, remnant Atlantic white cedar stand in Mississippi. In: Conner WH, Doyle TW, Krauss KW (eds) Ecology of tidal freshwater forested wetlands of the Southeastern United States. Springer, Dordrecht, pp 89–111

Kim SC (2013) Evaluation of a three-dimensional hydrodynamic model applied to Chesapeake Bay through long-term simulation of transport processes. J Am Water Res Assoc:1–13. https://doi.org/10.1111/jawr.12113

Kirwan ML, Megonigal JP (2013) Tidal wetland stability in the face of human impacts and sea-level rise. Nature 504:53–60. https://doi.org/10.1038/nature12856

Kirwan ML, Guntenspergen GR, D'Alpaos A, Morris JT, Mudd SM, Temmerman S (2010) Limits on the adaptability of coastal marshes to rising sea level. Geophys Res Lett 37:L23401. https://doi.org/10.1029/2010GL045489

Krauss KW, Duberstein JA, Doyle TW, Conner WH, Day RH, Inabinette LW, Whitbeck JL (2009) Site condition, structure, and growth of bald cypress along tidal/non-tidal salinity gradients. Wetlands 29:505–519

Kuang C, Chen W, Gu J, Su TC, Song H, Ma Y, Dong Z (2017) River discharge contribution to sea level rise in the Yangtze River Estuary, China. Cont Shelf Res 134:63–75

Kurz H, Wagner KA (1957) Tidal marshes of the Gulf and Atlantic coasts of northern Florida and Charleston, South Carolina. Florida State University, Studies No. 24

Laderman AD (1989) The ecology of Atlantic white cedar wetlands: a community profile. Biological Report 85(7.21). U.S. Department of the Interior, Fish and Wildlife Service, Washington, DC

Langbein WB (1963) The hydraulic geometry of a shallow estuary. Bull Int Assoc Sci Hydrol 8:84–94

Larson M, Sato S (2017) Coastal hydrology, Chapter 86. In: Singh VP (ed) Handbook of hydrology, 2nd edn. McGraw Hill, New York

Light HM, Darst MR, Mattson RA (2007) Ecological characteristics of tidal freshwater forests along the lower Suwannee River, Florida. In: Conner WH, Doyle TW, Krauss KW (eds) Ecology of tidal freshwater forested wetlands of the Southeastern United States. Springer, Dordrecht, pp 291–320

Liu Y, Kumar M (2016) Role of meteorological controls on interannual variations in wet-period characteristics of wetlands. Water Resour Res 52:5056–5074. https://doi.org/10.1002/2015WR018493

Liu Z, Li F, Li N, Wang R, Zhang H (2016) A novel region-merging approach for coastline extraction from Sentinel-1A IW Mode SAR imagery. IEEE Geosci Remote Sens Lett 13 (3):324–328

Liu X, Conner WH, Song B, Jayakaran AD (2017) Forest composition and growth in a forested wetland community across a salinity gradient in South Carolina. For Ecol Manag 389:211–219

Lockaby BG, Walbridge MR (1998) Biogeochemistry. In: Messina MG, Conner WH (eds) Southern forested wetlands: ecology and management. Lewis Publishers, Boca Raton, FL, pp 149–172

Luan HL, Ding PX, Wang ZB, Ge JZ, Yang SL (2016) Decadal morphological evolution of the Yangtze Estuary in response to river input changes and estuary engineering projects. Geomorphology 266:12–23

Lugo AE, Brown S, Brinson MM (1988) Forested wetlands in freshwater and salt-water environments. Limnol Oceanogr 33:894–909

Macmillan DH (1966) Tides. American Elsevier Publishing Company, New York, p 240

Matthews JB, Matthews JBR (2014) Physics of climate change: harmonic and exponential processes from in situ ocean time series observations show rapid asymmetric warming. J Adv Phy 2:1137–1171. http://www.cirjap.com, japeditor@gmail.com
McLeod KW, McCarron JK, Conner WH (1996) Effects of flooding and salinity on photosynthesis and water relations of four southeastern coastal plain forest species. Wetl Ecol Manag 4:31–42
Meselhe EA, Habib EH (2005) Hydrologic investigation of low gradient watersheds. A final report submitted by University of Louisiana, Lafayette, LA to U.S. Army Research Office, Research Triangle Park, NC
Meybeck M (2003) Global analysis of river systems: from Earth system controls to Anthropocene 4 syndromes. Philos Trans R Soc B. https://doi.org/10.1098/rstb.2003.1379
Mitsch WJ, Gosselink JG (2000) Wetlands, 3rd edn. Wiley, New York
Mitsch WJ, Gosselink JG, Anderson CJ, Zhang L (2009) Wetland Ecosystems. Wiley, Hoboken, NJ
Moore JH, Carter JH (1987) Habitats of white cedar in North Carolina. In: Laderman AD (ed) Atlantic white cedar wetlands. Westview Press, Boulder, CO, pp 177–188
Morris JT, Sundareshwar PV, Nietch CT, Kjerfve B, Cahoon DR (2002) Responses of coastal wetlands to rising sea level. Ecology 83:2869–2877
Najjar RG, Walker HA, Anderson PJ, Barron EJ, Bord RJ, Gibson JR, Polsky CD (2000) The potential impacts of climate change on the mid-Atlantic coastal region. Clim Res 14(3):219–233
NOAA (National Oceanographic and Atmospheric Agency) (2017) Tides and currents map. https://tidesandcurrents.noaa.gov/gmap3/. Accessed 1 Nov 2017
Noe GB, Krauss KW, Lockaby BG, Conner WH, Hupp CR (2013) The effect of increasing salinity and forest mortality on soil nitrogen and phosphorus mineralization in tidal freshwater forested wetlands. Biogeochemistry 114:225–244
Noe GB, Hupp CR, Bernhardt CE, Krauss KW (2016) Contemporary deposition and long-term accumulation of sediment and nutrients by tidal freshwater forested wetlands impacted by sea level rise. Estuar Coasts 39:1006–1019
Nunziata F, Buono A, Migliaccio M (2016) A new look at the old sea oil slick observation problem: opportunities and pitfalls of SAR polarimetry. In: 2016 IEEE International Geoscience and Remote Sensing Symposium (IGARSS). Beijing, pp 4027–4030. https://doi.org/10.1109/IGARSS.2016.7730047
Nuttle WK, Hemond HF (1988) Salt marsh hydrology: implications for biogeochemical fluxes to the atmosphere and estuaries. Glob Biogeochem Cycles 2(2):91–114
Odum WE (1988) Comparative ecology of tidal freshwater and salt marshes. Annu Rev Ecol Syst 19:147–176
Odum WE, Smith TJ III, Hoover JK, McIvor CC (1984) The ecology of tidal freshwater marshes of the United States east coast: a community profile. Report FWS/OBS-83/17. U.S. Department of the Interior, Fish and Wildlife Service, Washington, DC
Oey LY (2005) A wetting and drying scheme for POM. Ocean Model 9(2):133–115. https://doi.org/10.1016/j.ocemod.2004.06.002
Oey LY, Ezer T, Hu C, Muller-Karger FE (2007) Baroclinic tidal flows and inundation processes in Cook, Inlet, Alaska: numerical modeling and satellite observation. Ocean Dyn 57:205–221
Officer CB (1976) Physical oceanography of estuaries (and associated coastal waters). Wiley, New York
Ozalp M, Conner WH, Lockaby BG (2007) Above-ground productivity and litter decomposition in a tidal freshwater forested wetland on Bull Island, SC, USA. For Ecol Manag 245:31–43
Patchineelam SM, Kjerfve B (2004) Suspended sediment variability on seasonal and tidal time scales in the Winyah Bay estuary, South Carolina, USA. Estuar Coast Shelf Sci 59:307–318
Perry L, Williams K (1996) Effects of salinity and flooding on seedlings of cabbage palm (*Sabal palmetto*). Oecologia 105:428–434
Pezeshki SR, DeLaune RD, Patrick WH (1987) Response of bald cypress (*Taxodium distichum* L. var. *distichum*) to increases in flooding salinity in Louisiana's Mississippi River Deltaic Plain. Wetlands 7:1–10

Pierfelice KN, Lockaby BG, Krauss KW, Conner WH, Noe GB, Ricker MC (2017) Salinity influences on above- and belowground net primary productivity in tidal wetlands. J Hydrol Eng 22(1):D5015002. https://doi.org/10.1061/(ASCE)HE.1943-5584.0001223

Rheinhardt R (1992) A multivariate analysis of vegetation patterns in tidal freshwater swamps of lower Chesapeake Bay, USA. Bull Torrey Bot Club 119:192–207

Samadi S, Tufford DL, Carbone GJ (2017) Assessing parameter uncertainty of a semi-distributed hydrology model for a shallow aquifer dominated environmental system. J Am Water Res Assoc 53:1368–1389. https://doi.org/10.1111/1752-1688.12596

Savenije HHG (1992) Lagrangian solution of St. Venant's equations for alluvial estuary. J Hydraul Eng 118:1153–1163

Savenije HHG (2005) Salinity and tides in alluvial estuaries. Elsevier, Amsterdam

Savenije HHG (2015) Prediction in ungauged estuaries: an integrated theory. Water Resour Res 51:2464–2476. https://doi.org/10.1002/2015WR016936

Savenije HHG, Toffolon M, Haas J, Veling EJM (2008) Analytical description of tidal dynamics in convergent estuaries. J Geophys Res 113:C10025. https://doi.org/10.1029/2007JC004408

Shaffer GP, Perkins TE, Hoeppner S, Howell S, Benard H, Parsons AC (2003) Ecosystem health of the Maurepas Swamp: feasibility and projected benefits of a freshwater diversion. Final Report. Environmental Protection Agency Region 6, Dallas, TX

Shaffer GP, Wood WB, Hoeppner SS, Perkins TE, Zoller J, Kandalepas D (2009) Degradation of baldcypress—water tupelo swamp to marsh and open water in southeastern Louisiana, U.S.A.: an irreversible trajectory? J Coast Res Spec Issue 54:152–165

Sharitz RR, Mitsch WJ (1993) Southern floodplain forests. In: Martin WH, Boyce SG, Echternacht AC (eds) Biodiversity of the Southeastern United States: lowland terrestrial communities. Wiley, New York, pp 311–372

Song D, Wang XH, Zhu X, Bao X (2013) Modelling studies of the far field effects of tidal flat reclamation on tidal dynamics in the East China Sea. Estuar Coast Shelf Sci 133:147–160

Teas HJ (2013) Ecology and biology of mangroves. Springer Science and Business Media, Dordrecht

Thompson JR, Sorenson HR, Gavin H, Refsgaard A (2004) Application of the coupled MIKESHE/MIKE 11 modelling system to a lowland wet grassland in southeast England. J Hydrol 293:151–179

Tomlinson PB (2016) The botany of mangroves, 2nd edn. Cambridge University Press, London

Torres R (2017) Channel geomorphology along fluvial-tidal transition, Santee River, USA. Geol Soc Am Bull 129:1681–1691. https://doi.org/10.1130/B31649

Torres R, Goni MA, Voulgaris G, Lovell CR, Morris JT (2004) Effects of low tide rainfall on intertidal zone material cycling, Chapter 6. In: The Ecomorphology of Tidal Marshes, Coastal and Estuarine Studies 59, American Geophysical Union, pp 93–114. https://doi.org/10.1029/59CE07

Twilley RR, Chen R (1998) A water budget and a hydrology model of a basin mangrove forest in Rookery Bay in Florida. Mar Freshw Res 49:309–323

Twilley RR, Day JW (2012) Mangrove wetlands. In: Day JW, Crump BC, Kemp WM, Yáñez-Arancibia A (eds) Estuarine Ecology, 2nd edn. Wiley, Hoboken, NJ. https://doi.org/10.1002/9781118412787.ch7

Twilley RR, R-Monroy VH (2005) Developing performance measures of mangrove wetlands using simulation models of hydrology, biogeochemistry, and community dynamics. J Coast Res SI40:79–93

USACOE (2017) Charleston Harbor, SC, Regional Sediment Management study; beneficial use of dredged material through nearshore placement. Prepared by ERDC/CHL as Final Report # TR-17-7 in May 2017 for U.S. Army Corps of Engineers, Washington, DC, 20314-1000

USGS, United States Geologic Survey (2017) Current water data for the nation. Station 02135200, Pee Dee River at Hwy 701 near Bucksport SC. https://waterdata.usgs.gov/sc/nwis/uv?site_no=02135200. Accessed 11 Nov 2017

Vörösmarty CJ, McIntyre PB, Gessner MO, Dudgeon D, Prusevich A, Green P, Davies PM (2010) Global threats to human water security and river biodiversity. Nature 467(7315):555–561

Williams K, Ewel KC, Stumpf RP, Putz FE, Workman TW (1999a) Sea-level rise and coastal forest retreat on the west coast of Florida, USA. Ecology 80:2045–2063

Williams K, Pinzon ZS, Stumpf RP, Raabe EA (1999b) Sea-level rise and coastal forests on the Gulf of Mexico. US Geological Survey. Open-File Report 99-441

Williams K, MacDonald M, McPherson K, Mirti TH (2007) Ecology of the coastal edge of hydric hammocks on the Gulf coast of Florida. In: Conner WH, Doyle TW, Krauss KW (eds) Ecology of tidal freshwater forested wetlands of the Southeastern United States. Springer, Dordrecht, pp 255–289

Williams TM, Chow AT, Song B (2012) Historical visualization evidence on forest salt marsh transition in Winyah Bay, South Carolina: a retrospective study in sea level rise. Wetland Sci Pract 29:5–17

Wolanski E (2007) Estuarine ecohydrology. Elsevier, Amsterdam

Wolaver TG, Dame RF, Spurrier JD, Miller AB (1988) Bly Creek ecosystem study – inorganic sediment transport within a euhaline salt marsh basin, North Inlet, South Carolina. J Coast Res 4:607–615

Woodruff JD, Irish JL, Camargo SJ (2013) Coastal flooding by tropical cyclones and sea level rise. Nature 504:44–52. https://doi.org/10.1038/nature12855

Wu K, Johnson CA (2008) Hydrologic comparison between a forested and wetland/lake dominated watershed using SWAT. Hydrol Process 22:1431–1442

Wu K, Xu YJ (2006) Evaluation of the applicability of the SWAT model for coastal watersheds in southeastern Louisiana. J Am Water Resour Assoc 42(5):1247–1260

WWAP (World Water Assessment Programme) (2009) Water in a changing world. The Third 6 World Water Development Report. UNESCO, Paris

Xiao C, Zhang K, Shen J (2006) CEST: a three-dimensional coastal and estuarine storm tide model. International Hurricane Research Center, Florida International University, Miami, FL, p 20

Yang SL, Milliman JD, Xu KH, Deng B, Zhang XY, Luo XX (2014) Downstream sedimentary and geomorphic impacts of the Three Gorges Dam on the Yangtze River. Earth Sci Rev 138:469–486

Young PJ, Keeland BD, Sharitz RR (1995) Growth response of bald cypress [*Taxodium distichum* (L.) Rich.] to an altered hydrologic regime. Am Midl Nat 133:206–212

Zhang RS (1984) The formation of the Yellow River delta and the coastal plain of northern Jiangsu. Acta Geograph Sin 39(2):173–184. (In Chinese with English abstract)

Zhang T, Yang X, Hu S, Su F (2013) Extraction of coastline in aquaculture coast from multispectral remote sensing images: object-based region growing integrating edge detection. Remote Sens 5(9):4470–4487